arXiv:1402.2348v1 [physics.atom-ph] 11 Feb 2014

Attosecond time delay in the photoionization of endohedral atoms A@C_{60}: A new probe of confinement resonances

P. C. Deshmukh[†‡], A. Mandal[†], S. Saha[†], A. S. Kheifets[⋆], V. K. Dolmatov[♭] and S T Manson[♯]
[†]*Department of Physics, Indian Institute of Technology Madras, Chennai-600036, India*
[‡]*Department of Physics, CPGS, Jain University, Bangalore, 560011, India*
[⋆]*Research School of Physics and Engineering, The Australian National University, Canberra ACT 0200, Australia*
[♭] *Department of Physics and Earth Science, University of North Alabama, Florence, AL 35632, USA and*
[♯]*Department of Physics and Astronomy, Georgia State University, Atlanta, GA 30303, USA*
(Dated: February 12, 2014)

The effects of confinement resonances on photoelectron group delay (Wigner time delay) following ionization of an atom encapsulated inside a C_{60} cage have been studied theoretically using both relativistic and non-relativistic random phase approximations. The results indicate clearly the resonant character of the confinement oscillations in time delay of the $4d$ shell of Xe@C_{60} and present a most direct manifestation of Wigner time delay. These oscillations were missed in a previous theoretical investigation of Ar@C_{60} [PRL **111**, 203003 (2013)].

PACS numbers: 32.80.Rm 32.80.Fb 42.50.Hz

Unprecedented advances in experimental techniques in measuring time intervals at the attosecond level [1] have engendered the ability to scrutinize the time delay in photoionization of atomic systems in the laboratory [2–4], thereby allowing us to probe the fundamental process of photoionization in the time domain. Specifically, using attosecond pulses of electromagnetic radiation, the time difference between the emergence of photoelectrons from two neighboring atomic subshells has been measured both in Ne [3] and Ar [4, 5]. These experimental results have stimulated a host of theoretical calculations to explain and to further explore this phenomenon [6–9]. This is of great interest, not only as a new way to study a fundamental process of nature, but also as an outstanding, unique opportunity towards a deeper understanding of the most informative parameter of the process, the photoionization amplitude. This is because the time delay is related to the energy derivative of the phase of the amplitude driving the process [10]. Indeed, to date, the only method for getting the maximum experimental information on photoionization lies through a set of measurements of total and differential photoionization cross sections, but allows only the absolute values and relative phases of matrix elements to be deduced; this is known as a *complete photoionization experiment* [11]. Time delay investigations, however, go beyond the *complete experiment* strategy and yield the derivative of the phase with respect to the photoelectron energy. Time delay investigations, thus, provide a new avenue to discern the characteristics of the basic physical quantity - the photoionization amplitude - and, thus, of the photoionization phenomenon itself. It is the ultimate aim of this paper to promote the expansion of time delay studies towards situations where they have not yet been exploited and where novel effects might occur - to atoms under confinement.

The theory of time delay in physics was developed some time ago [12] and was originally envisioned as a way to study resonances - the temporary trapping of one (or more) electrons in a quasi-bound state or a potential well. Indeed, the Breit-Wigner formula of resonant scattering $\tau = 2/\Gamma$ equates the time delay τ with the resonant width Γ at half maximum of the cross-section [13]. Resonances are ubiquitous in photoionization of atoms, and these resonances can be of different natures: inner-shell excitations, two-electron excitations, shape resonances, etc. Of great recent interest to investigators, which has shaped an area of extremely active modern research activities [14], have been studies of a new genre of resonances, termed confinement resonances, that occur in the photoionization of an atom A trapped at the center of a C_{60} molecule, the $A@C_{60}$ endohedral atom. The phenomenon of confinement resonances was predicted theoretically long ago (see, e.g., [15]). However, it is only fairly recently that confinement resonances have been studied in depth in numerous theoretical studies at various levels of sophistication (see [16–19] and references therein), and only very recently verified experimentally in the photoionization of endohedral atoms [20, 21]. Confinement resonances have been explained as interferences between the photoelectron wave emitted directly, and those that experience one or more scattering off the walls of the encapsulating fullerene [22].

If this understanding is correct, these multiple scatterings should show up prominently in the time delay of the photoelectron relative to the time delay of the free atom. It is, however, not at all clear beforehand as to what degree time delay of atomic photoionization is modified by confining an atom inside of C_{60} compared to the free atom. Moreover, a recent theoretical study of time delay in Ar@C_{60} [23] have not revealed any confinement resonances in the time delay at all. At the same time, confinement resonances were clearly seen in time delay of a model system He^+@C_{60} [24]. This system, however, was unstable and the theoretical analysis was performed on a one-electron level. We are, therefore, presented with the task of unraveling the confinement resonances in a realistic atomic system taking full account of many-electron effects, thereby significantly enlarging upon the previous

studies [23, 24].

In this Letter, we explore photoionization of the $4d$ subshell of Xe@C_{60} , where confinement resonances have been found experimentally [20, 21]. Specifically, we focus upon how the time delay can be used to characterize the confinement resonances, along with the time delay phenomenology produced by the resonances. A model potential is employed to introduce the effects of the confining C_{60} on the encaged Xe atom. In this model, the C_{60} cage is approximated by an attractive spherical square well potential of certain inner radius $R_{\rm inner}$, thickness Δ, and depth U_0:

$$V(r) = \begin{cases} -U_0 < 0 & \text{if } R_{\rm inner} \le r \le R_{\rm inner} + \Delta \\ 0 & \text{otherwise.} \end{cases} \quad (1)$$

This should be adequate because the $4d$ subshell is so deeply bound that it cannot hybridize with any of the levels of C_{60} , and the photon energy range (80 to 160 eV) is well away from the C_{60} plasmons so that interchannel coupling with atomic photoionization is not important. Furthermore, recent photoionization calculations employing such a model resulted in rather good agreement with the experimental confinement resonances [21]. To properly account for correlations, the calculations are performed within the framework of the random-phase approximation (RPA), both the non-relativistic [25] and relativistic [26] versions. This has the advantages of spotlighting any relativistic effects.

The time delay is calculated from the photoionization amplitude as $\tau = d \arg f(E)/dE \equiv \mathrm{Im}\Big[f'(E)/f(E)\Big]$. The amplitude $f(E)$ is given by the partial wave expansion as

$$f(E) \propto \sum_{l=l_i\pm1} e^{i\delta_l} i^{-l} Y_{lm}(\hat{k})\,(-1)^m \begin{pmatrix} l & 1 & l_i \\ -m & 0 & m_i \end{pmatrix} \times \langle El \| D \| n_i l_i \rangle \quad (2)$$

evaluated in the $\hat{z}$ direction of the polarization axis of light. In the non-relativistic RPA method, the reduced dipole matrix element $\langle El \| D \| n_i l_i \rangle$ is evaluated by solving a set of integro-differential equations [25] exhibited graphically by diagrams of Fig. 1. In the absence of inter-shell correlation, the dipole matrix element is represented by the left-most diagram which corresponds to the photon absorption and electron emission from the same shell. The inter-shell correlation allows for the photon absorption by the shell $n_j l_j$ and the electron emission from the shell $n_i l_i$. This process is shown by the two remaining diagrams in which the inter-shell correlation precedes or follows the photon absorption (time-reverse and time-forward diagrams, respectively). The exchange leads to the two ladder-type diagrams (not shown) in addition to the two bubble-type diagrams shown in Fig. 1.

The same matrix element is used to evaluate the partial photoionization cross-section from an occupied state $n_i l_i$ to the photoelectron continuum state El

$$\sigma_{n_i l_i \to El}(\omega) = \frac{4}{3}\pi^2 \alpha a_0^2 \omega \left| \langle El \,\| D \| n_i l_i \rangle \right|^2 . \quad (3)$$

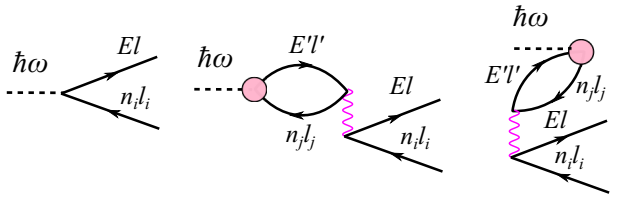

FIG. 1: (Color online) Graphical representation of the RPA Equations [25]. Left: non-correlated dipole matrix element. Center: time-forward process. Right: time-reverse process.

Here α is the fine structure constant and a_0 is the Bohr radius. The occupied orbitals $n_i l_i$ and continuous orbitals El are obtained by the self-consistent field and frozen-core field Hartree-Fock methods, respectively, as in Ref [25]. For the present case of the $4d$ shell in Xe, correlations with the $5s$ and $5p$ shells are included resulting in 5 non-relativistic channels. The relativistic RPA (RRPA) method, is exactly the same as the nonrelativistic version, except that it is based on the fully relativistic Dirac equation, rather than the Schrödinger equation, and Dirac-Fock [27] instead of Hartree- Fock orbitals are employed. In the present RRPA calculation, final state correlations are included through interchannel coupling between all the 13 relativistic dipole channels originating in the $5p$, $5s$ and $4d$ subshells which are open for photoionization in the energy range studied in the present work; in other words with the relativistic splittings of the five nonrelatistic channels become thirteen channels. Omitting the inner shells has no significant effect upon the results. In both cases, the fullerene cage is modeled by a square-well potential (1) with the following parameters: $R_{\rm inner} = 5.8$ a.u., $\Delta = 1.9$ a.u., and $U_0 = 0.302$ au.

The results of the calculations are shown in Fig. 2. In the upper panels, the $4d$ partial photoionization cross-sections for the free (left) and confined (right) Xe atoms are displayed. The RRPA results are shown for the spin-resolved $4d_{1/2}$ and $4d_{3/2}$ subshells leading to the ϵf ionization continuum. The cross-sections are weighted with the inverse statistical factors (5/2 and 5/3) to facilitate the shape comparison. The RPA results are shown for the $4d \to \epsilon f$ and $4d \to \epsilon p$ transitions; the former is clearly dominant in the given energy region. This allows us to concentrate on the cross-section and time delay analysis in the dominant channel only. The RPA and RRPA cross-section results are very close for the free Xe atom after a small photon energy adjustment is made to accommodate different $4d$ ionization thresholds in RRPA (theoretical) and RPA (experimental). The cross-sections for Xe@C_{60} are qualitatively similar between the two methods, although the RPA predicts somewhat sharper resonances at lower photon energy end. This difference between RPA and RRPA occurs owing to the interchannel coupling among the spin-orbit-split relativistic channels which tends to dampen the confinement resonances a bit. This is known as spin-orbit-activated interchannel coupling [28, 29].

In the lower panels, the Wigner time delay results for free (left) and confined (right) Xe atoms are shown. Agreement of the two methods for the free Xe atom are good except for lower photon energy end where one sees a strong deviation between the spin-resolved $4d$ states; again this is caused by the spin-orbit-activated interchannel coupling. The RPA delay is close to the RRPA $4d_{3/2} \rightarrow \epsilon f_{5/2}$ delay. For $Xe@C_{60}$, the two methods show the same set of confinement resonances. The precise shape of the lowest resonance is somewhat dependent of the spin-orbit splitting and the interchannel coupling.

Of particular importance is the finding that the confinement resonances are much more prominent in the time delay than in the cross-section, thus making time-delay studies a much more sensitive probes of confinement resonances. In addition, the maxima in the time delay are not at the same energies as the maxima in the cross-sections. This is not completely surprising because the the cross-section is quadratic with the amplitude, and the time delay is calculated from the logarithmic derivative of the amplitude.

A more detailed comparison of the cross-sections and time delays in free and encapsulated Xe atoms is shown in Fig. 3; for simplicity, only the nonrelativistic RPA result is shown since the RRPA results are qualitatively similar. In the upper panel of this figure, the normalized cross-section difference $[\sigma(Xe@C_{60}) - \sigma(Xe)]/\sigma(Xe)$ is plotted and compared with the experimental data of [21]. Our RPA calculation qualitatively reproduces all the resonances seen experimentally. A small offset in peak position of the resonances may be attributed to the rough spherical-well representation of the fullerene cage in the present work. In the bottom panel, an analogous plot for the time delay difference $\tau(Xe@C_{60}) - \tau(Xe)$ is displayed. In this difference representation, the oscillations on both plots are perfectly aligned, i.e.' the maima and minima in cross-section space and time-delay space occur at exactly the same energies.

Note also that, for both free and confined Xe, the three relativistic $4d \rightarrow \epsilon f$ channels exhibit rather different time delays for energies near the thresholds. This is an indication that there are real dynamical differences among the channels brought about by interchannel coupling. With increasing energy, these differences are seen to disappear, and the time delays for all three relativistic channels coalesce; not only do they coalesce with one another, but they also become indistinguishable from the nonrelativistic result. This occurs because the spin-orbit-activated interchannel coupling decreases as the energy increases because the small difference in thresholds becomes irrelevant as the photoelectron energy gets much larger than the spin-orbit splitting [28, 29].

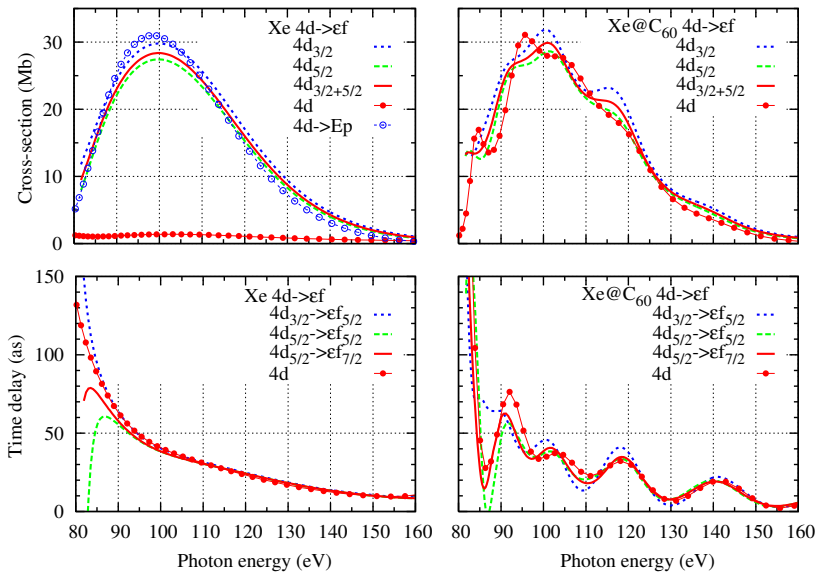

FIG. 2: Top: partial photoionization cross-sections of the $4d$ shell in Xe (left) and $Xe@C_{60}$ (right). The RRPA calculations for spin-orbit resolved components $4d_{3/2}$ ($\times 5/2$), $4d_{5/2}$ ($\times 5/3$) and their sum are drawn with lines. The RPA calculations for the $4d \rightarrow \epsilon f$ and $4d \rightarrow \epsilon p$ (left panel only) cross-sections are drawn with line-dots. Bottom: time delay in photoionization of the $4d \rightarrow \epsilon f$ channel of Xe (left) and $Xe@C_{60}$ (right). The RRPA calculations for various spin-orbit resolved components are drawn with lines while the RPA calculation is drawn with line-dots .

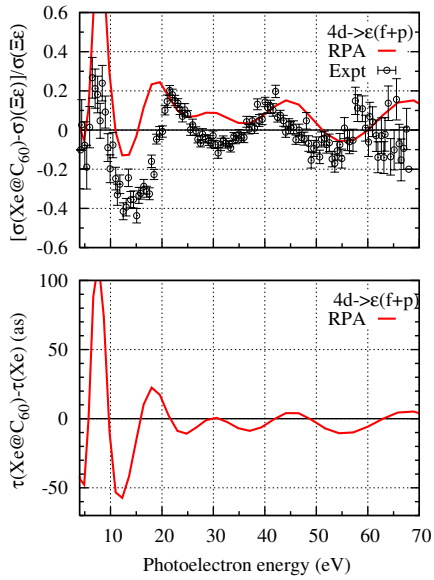

FIG. 3: Normalized photoionization cross-section difference $[\sigma(Xe@C_{60}) - \sigma(Xe)]/\sigma(Xe)$ (top) and time delay difference $\tau(Xe@C_{60}) - \tau(Xe)$ (bottom) as functions of photoelectron energy. The RPA calculation is shown with a solid line. The experimental data in the top panel are from [21].

In conclusion, in the present work, we have demonstrated clear presence of confinement resonances in photoelectron group delay (Wigner time delay) of the $4d$ shell of endohedrally confined Xe atom. These resonances have been observed recently in the $4d$ photoionization cross-section of Xe@C_{60} [20, 21]. Our calculations show that these resonances are even more prominent in the time delay. This suggests that additional insights into the photoionization process can be obtained by investigations performed in time-delay space. We further suggest that time delay experiment be used as an effective novel way to study photoionization not only of neutral endohedral A@C_{60} but their charged members A@$C_{60}^{\pm z}$ as well as giant A@$C_{n>60}$ and multi-walled A@C_{60}@C_{240}, A@C_{60}@C_{240}@C_{540}, *etc.*, endohedral fullerenes, each of which exhibits its own specific photoionization properties [18]. Also of interest are studies of time delays of other elementary processes involving endohedral fullerenes, e.g., elastic electron scattering off A@C_{60}, where initial insight has been provided recently [30].

We note that in the present work we did not consider the influence of the probing IR field on the measured time delay. This effect, however, was analyzed in [24] where it was found that the laser Coulomb coupling correction and the screening effect of the C_{60} shell nearly totally cancel each other and hence the measured time delay will be essentially the Wigner time delay.

Finally, we urge experimentalists to initiate time delay studies of endohedral fullerenes for which the well established attosecond streaking [3] and RABITT [4] techniques could prove to be useful.

This work was supported by the Department of Science and Technology (DST), Government of India, by the National Science Foundation, by the Department of Energy, Office of Chemical Sciences, and by the Australian Research Council.

[1] A. Baltuška *et al*, *Attosecond control of electronic processes by intense light fields*, Nature **421**, 611 (2003).

[2] P. Eckle *et al*, *Attosecond ionization and tunneling delay time measurements in helium*, Science **322**(5907), 1525 (2008).

[3] M. Schultze *et al*, *Delay in Photoemission*, Science **328**(5986), 1658 (2010).

[4] K. Klünder *et al*, *Probing single-photon ionization on the attosecond time scale*, Phys. Rev. Lett. **106**(14), 143002 (2011).

[5] D. Guénot, K. Klünder, C. L. Arnold, D. Kroon, J. M. Dahlström, M. Miranda, T. Fordell, M. Gisselbrecht, P. Johnsson, J. Mauritsson, et al., *Photoemission-time-delay measurements and calculations close to the 3s-ionization-cross-section minimum in ar*, Phys. Rev. A **85**, 053424 (2012).

[6] V. S. Yakovlev, J. Gagnon, N. Karpowicz, and F. Krausz, *Attosecond streaking enables the measurement of quantum phase*, Phys. Rev. Lett. **105**(7), 073001 (2010).

[7] A. S. Kheifets and I. A. Ivanov, *Delay in atomic photoionization*, Phys. Rev. Lett. **105**(23), 233002 (2010).

[8] M. Ivanov and O. Smirnova, *How accurate is the attosecond streak camera?*, Phys. Rev. Lett. **107**, 213605 (2011).

[9] R. Pazourek, J. Feist, S. Nagele, and J. Burgdörfer, *Attosecond streaking of correlated two-electron transitions in helium*, Phys. Rev. Lett. **108**, 163001 (2012)

[10] C. A. A. de Carvalho and H. M. Nussenzveig, *Time delay*, Phys. Rep. **364**(2), 83 (2002.

[11] N. A. Cherepkov and S. K. Semenov, *On a complete experiment on photoionization of atoms*, J. Phys. B **37**(6), 1267 (2004).

[12] E. P. Wigner, *Lower limit for the energy derivative of the scattering phase shift*, Phys. Rev. **98**(1), 145 (1955).

[13] R. G. Newton, *Scattering Theory of Waves and Particles* (Courier Dover Publications, 1982).

[14] M. Saunders, H. A. Jiménez-Vázquez, R. J. Cross, and R. J. Poreda, *Stable compounds of helium and neon: He@C_{60} and Ne@C_{60}*, Science **259**(5100), 1428 (1993).

[15] M. J. Puska and R. M. Nieminen, *Photoabsorption of atoms inside C_{60}*, Phys. Rev. A **47**, 1181 (1993).

[16] M. Y. Amusia, A. S. Baltenkov, L. V. Chernysheva, Z. Felfli, and A. Z. Msezane, *Dramatic distortion of the 4d giant resonance by the C_{60} fullerene shell*, J. Phys. B **38**(10), L169 (2005).

[17] V. K. Dolmatov and S. T. Manson, *Correlation confinement resonances in photoionization of endohedral atoms: Xe@C_{60}*, J. Phys. B **41**(16), 165001 (2008).

[18] V. K. Dolmatov, *Photoionization of atoms encaged in spherical fullerenes*, Adv. Quant. Chem. **58**, 13 (2009).

[19] M. E. Madjet, T. Renger, D. E. Hopper, M. A. McCune, H. S. Chakraborty, J.-M. Rost, and S. T. Manson, *Photoionization of Xe inside C_{60}: Atom-fullerene hybridization, giant cross-section enhancement, and correlation confinement resonances*, Phys. Rev. A **81**, 013202 (2010).

[20] A. L. D. Kilcoyne, A. Aguilar, A. Müller, S. Schippers, C. Cisneros, G. Alna'Washi, N. B. Aryal, K. K. Baral, D. A. Esteves, C. M. Thomas, et al., *Confinement resonances in photoionization of Xe@C_{60}^+*, Phys. Rev. Lett. **105**, 213001 (2010).

[21] R. A. Phaneuf, A. L. D. Kilcoyne, N. B. Aryal, K. K. Baral, D. A. Esteves-Macaluso, C. M. Thomas, J. Hellhund, R. Lomsadze, T. W. Gorczyca, C. P. Ballance, et al., *Probing confinement resonances by photoionizing Xe inside a C_{60}^+ molecular cage*, Phys. Rev. A **88**, 053402 (2013).

[22] J. Luberek and G. Wendin, *The Ba 4d-f giant dipole resonance as a probe of the structure of endohedral Ba@C_n metallofullerenes*, Chem. Phys. Lett. **248**(34), 147 (1996).

[23] G. Dixit, H. S. Chakraborty, and M. Madjet, *Time delay in the recoiling valence photoemission of Ar endohedrally confined in C_{60}*, Phys. Rev. Lett. **111**, 203003 (2013).

[24] S. Nagele, R. Pazourek, M. Wais, G. Wachter, and J. Burgdörfer, *Time-resolved photoemission using attosecond streaking*, J. Phys. Conf. Ser. arXiv 1401.6328 (2014).

[25] M. I. Amusia and L. V. Chernysheva, *Computation of atomic processes : A handbook for the ATOM programs*

(Institute of Physics Pub., Bristol, UK, 1997).

[26] W. R. Johnson and C. D. Lin, *Multichannel relativistic random-phase approximation for the photoionization of atoms*, Phys. Rev. A **20**, 964 (1979).

[27] I. P. Grant, B. J. McKenzie, P. H. Norrington, D. F. Meyers, and N. C. Pyper, *An atomic multiconfigurational Dirac-Fock package*, Comp. Phys. Comm. **21**, 207 (1980).

[28] M. Y. Amusia, L. V. Chernysheva, S. T. Manson, A. M. Msezane, and V. Radojevi, *Strong electron correlation in photoionization of spin-orbit doublets*, Phys. Rev. Lett. **88**, 093002 (2002).

[29] S. S. Kumar, T. Banerjee, P. C. Deshmukh, and S. T. Manson, *Spin-orbit-interaction activated interchannel coupling in dipole and quadrupole photoionization*, Phys. Rev. A **79**, 043401 (2009).

[30] V. K. Dolmatov, M. B. Cooper, and M. E. Hunter, *Electron elastic scattering off endohedral fullerenes A@C60: The initial insight*, ArXiv e-prints (2014), 1401.2632.